Available online at www.sciencedirect.com
ScienceDirect
Organic Geochemistry 38 (2007) 1341–1355
Organic Geochemistry
www.elsevier.com/locate/orggeochem

Petroleum charge history in the Lunnan Low Uplift, Tarim Basin, China – Evidence from oil-bearing fluid inclusions

Se Gong [a,d,*], Simon C. George [b], Herbert Volk [a], Keyu Liu [c], Ping'an Peng [d]

[a] CSIRO Petroleum, P.O. Box 136, North Ryde, NSW 1670, Australia
[b] Australian Centre for Astrobiology, Macquarie University, Sydney, NSW 2109, Australia
[c] CSIRO Petroleum, P.O. Box 1130, Bentley, WA 6102, Australia
[d] State Key Laboratory of Organic Geochemistry, Guangzhou Institute of Geochemistry, Chinese Academy of Sciences, Guangzhou 510640, China

Received 10 September 2006; received in revised form 18 February 2007; accepted 26 February 2007
Available online 15 March 2007

Abstract

The petroleum charge history in the Lunnan Low Uplift (Tarim Basin, China) was investigated by comparing the geochemical characteristics of fluid inclusion (FI) oils from Ordovician and Triassic reservoirs with crude oils from stratigraphically different reservoirs. Quantitative Grain Fluorescence (QGF) and Total Scanning Fluorescence (TSF) were used to screen the reservoir samples so as to identify suitable samples for Molecular Composition of Inclusion (MCI) analysis. All of the samples contain C_{30} *n*-propylcholestanes, diagnostic of marine source rocks. The Ordovician-hosted FI oils differ from the Triassic-hosted FI oils, having higher relative abundances of C_{19} tricyclic terpane, C_{24} tetracyclic terpane and rearranged hopanes (Ts and C_{29} Ts), and higher Pr/Ph ratios, while the Triassic-hosted FI oils have lower Pr/Ph ratios and higher relative abundances of C_{23} tricyclic terpane, arylisoprenoids, 25-norhopanes and C_{35} homohopane. Several of the crude oils are similar to the Triassic-hosted FI oils. Based on the geochemical characteristics of the FI and crude oils combined with information on the burial history of the area, at least two petroleum charge episodes can be distinguished in the Lunnan Low Uplift. An early charge represented by the Ordovician-hosted FI oils was biodegraded, as evidenced by the presence of 25-norhopanes in the Triassic-hosted FI oils and crude oils but not in the Ordovician-hosted FI oils. Ordovician-hosted FI oils provide the only evidence for oil generated from Cambrian-Lower Ordovician source rocks. Triassic-hosted FI oils and crude oils in the Ordovician, Carboniferous and Triassic reservoirs are mixtures of biodegraded oil from an early charge episode, and more mature oil from later charge.

1. Introduction

The Lunnan Low Uplift is part of the Tabei Uplift in the Tarim Basin, a complex basin situated in northwestern China and one of the largest intermontane basins in the world (Graham et al., 1990) (Fig. 1). This area has undergone a range of tectonic events, which resulted in multiple stages of hydrocarbon generation, accumulation, destruction and re-migration (Huang et al., 1999; Li et al., 2000; Xiao et al., 2000; Yang et al., 2003). Petroleum types include normal,

* Corresponding author. Address: CSIRO Petroleum, P.O. Box 136, North Ryde, NSW 1670, Australia.
E-mail address: Se.Gong@csiro.au (S. Gong).

0146-6380/$ - see front matter © 2007 Elsevier Ltd. All rights reserved.
doi:10.1016/j.orggeochem.2007.02.014

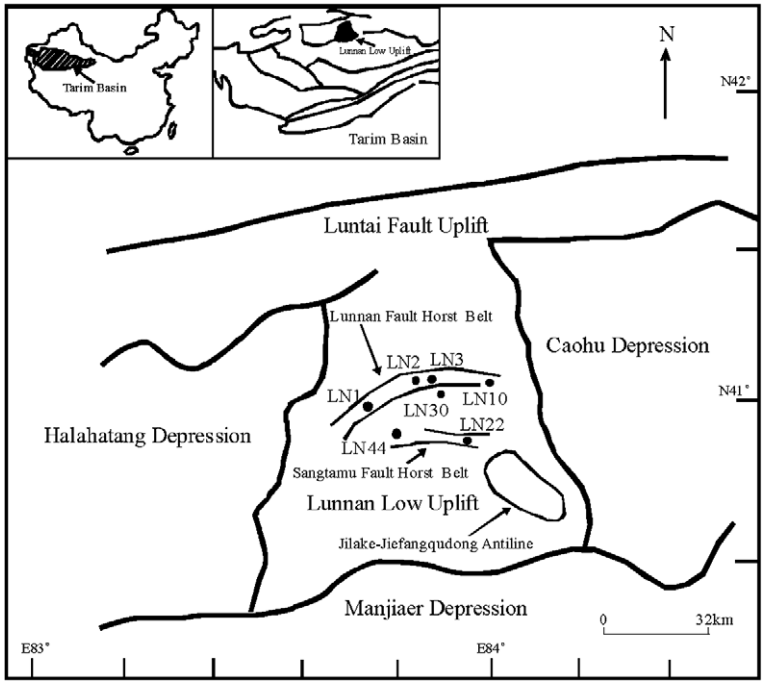

Fig. 1. Sketch maps showing the location of the Tarim Basin in China and the Lunnan Low Uplift in the Tarim Basin (index maps), and the structural outline of the Lunnan Low Uplift. Locations of the wells investigated in this study are shown by filled circles. Solid lines represent major faults.

heavy and high-wax oils, condensates and gas accumulations (Zhou and Zhang, 2000), reflecting the complex evolution of this region.

Although, numerous studies have been carried out in the last two decades, there is still much ongoing debate about the source rock and charge history of the Palaeozoic oils. Two sets of strata (Cambrian-Lower Ordovician and Middle-Upper Ordovician) are thought to be the source rocks of the Ordovician-Triassic reservoired oils in this region (Graham et al., 1990), but their relative importance remains controversial. Based on an oil/source study in the Tabei Uplift, it was concluded that crude oil in the Tarim Basin mainly originated from the Cambrian-Lower Ordovician source rocks (Zhao et al., 1997). He et al. (2002) attributed variation of petroleum properties in the Lunnan Low Uplift to effects of post-generation processes such as biodegradation and oxidation on Cambrian-Lower Ordovician-derived oils, based on consideration of the burial history of potential source rocks and homogenisation temperatures of oil inclusions in the reservoir. This interpretation is supported by studies on arylisoprenoid distributions (Sun et al., 2003; Wang et al., 2003). Other researchers argue that Middle-Upper Ordovician strata were the main effective source rocks. For example, Zhang et al. (2000, 2002, 2005) concluded that oils in Ordovician-Triassic reservoirs from the Tarim Basin had similar biomarker characteristics and originated from Middle-Upper Ordovician source rock. A similar conclusion was drawn by Hanson et al. (2000). We and other authors believe that mixing and multiple charge episodes have complicated the results of these oil-source rock correlation studies (Peng and Lü, 2002; Wang et al., 2003).

The charge history of the Lunnan Low Uplift still remains unclear. Li et al. (1999) suggested that there were three reservoir filling stages (Early Devonian, Early Permian and Tertiary, and two phases of uplift, erosion and re-migration at the end of the Devonian and the Permian. In contrast, Gu et al. (1998) held the opinion that Lunnan Low Uplift had five charge episodes: Late Devonian, Carboniferous, Jurassic, Cretaceous and Cenozoic, based on the thermal maturity history of the source rock generating the hydrocarbons, the genetic types of oil and gas, and reservoir bitumen analysis.

Oil trapped in fluid inclusions (FI) commonly occurs in petroleum reservoirs and along migration pathways, and is not affected by later alteration, such as mixing, biodegradation, and water washing.

In contrast, oil in reservoirs commonly consists of mixtures affected by processes occurring during petroleum generation, migration, trapping and subsequent alteration (England et al., 1987; Head et al., 2003). Hence, it is difficult to perform oil–source rock correlations and reconstruct the charge history of a petroleum reservoir using only the oil samples from the present petroleum reservoir. Oil in inclusions can aid interpretations of complex charge histories (Karlsen et al., 1993; George et al., 1997a, 1998a, in press). In addition, the geochemical characteristics of oil in inclusions can provide useful data to describe the source and thermal maturity of palaeo-oil during early charge episodes (Isaksen et al., 1998; George et al., 1997b).

In this study, FI oils were analysed to provide more rigorous data on the source rock for oils in Ordovician-Triassic reservoirs in the Lunnan Low Uplift. Charge history was reconstructed by combining the geochemical characteristics and homogenisation temperatures of fluid inclusions with modelled burial history and hydrocarbon generation history.

Period	Lithology	Depositional environment	Petroleum system element
Quaternary	Sandstone, conglomerate	Continental	Overburden
Neogene	Upper part: grey to yellow silstone and mudstone Lower part: brown–red sandstone and mudstone		
Palaeogene	Brown, grey, yellow siltstone and mudstone		
Cretaceous	Brown, grey, yellow siltstone and mudstone		
Jurassic	Sandstone and mudstone		
Triassic	Interbeded conglomerate, mudstone and sandstone		Reservoir rock
Permian	Brown, yellow and red sandstone and mudstone	Transitional	
Carboniferous	Interbeded grey mudstone siltstone and sandstone		Source rock/ reservoir rock
Devonian	Yellow sandstone and mudstone	Marine	Reservoir rock
Silurian	Yellow sandstone and shale		
Middle–Upper Ordovician	Dark limestone and marl		Source rock
Lower Ordovician	Grey carbonate and shale, grey dolomite		Source rock/ reservoir rock
Cambrian	Grey carbonate and shale, grey dolomite		
Precambrian	Carbonate, shale and volcanic rocks		

Fig. 2. Stratigraphy of the Lunnan Low Uplift, Tarim Basin, China (modified from Zhang and Huang, 2005).

2. Geological setting

The Lunnan Low Uplift is linked to the Manjiaer depression in the south and joined to the Luntai Fault Uplift in the north (Fig. 1). To the west is the Halahatang depression, and to the east side is the Caohu depression. The Lunnan and Sangtamu fault-horst belt and the Jilake–Jiefangqudong anticline occur in this region.

The Lunnan area became an uplift in the end of the Early Ordovician due to the late Caledonian orogeny (Zhang, 2000), and then was transformed into a large-scale nose uplift during the Devonian when it was affected by the early Hercynian orogeny. During Carboniferous time, northward and northwestward overlapping deposition of sediments led to interbedded sandstones, shales and limestones. The Lunnan and Sangtamu fault-horst belt formed due to Permian east–west faulting, caused by the late Hercynian orogeny. There was marine/terrestrial transitional development during the Carboniferous and Permian and some small-scale fault activity during the Late Cretaceous. The basement of the basin tilted from south to north and formed the present-day uplifted structure during the Cenozoic period (Lü et al., 2004; He et al., 2002).

The stratigraphy of the Tarim Basin consists of several marine, continental and transitional sequences (Fig. 2). The Palaeozoic strata were deposited almost entirely in marine settings (Li et al., 1996; Jia and Wei, 2002). The Palaeozoic potential source rocks include Cambrian-Lower Ordovician lagoonal carbonate and mudstone, and the Middle-Upper Ordovician platform carbonate (Zhang and Huang, 2005). Due to the multiple tectonic movements in the Lunnan region, the Lower Ordovician strata form a buried-hill uplift structure, over which Middle-Upper Ordovician, Silurian and Devonian strata are generally absent. Carboniferous and Permian strata are absent in the axial region of the Lunnan Low Uplift. Mesozoic–Cenozoic rocks are the overlying strata, but the Triassic strata are locally absent. So far, the Lunnan, Sang-tamu, Jiefangqudong and Tahe oilfields and the Jilake condensate field have been discovered in the Lunnan region. Oils have mainly accumulated in four reservoir strata: Ordovician, Carboniferous, Triassic and Jurassic.

3. Samples and experimental procedures

Sandstone and carbonate samples containing FIs were collected from Ordovician and Triassic reservoir rocks in the Lunnan and Sangtamu fault-horst belts (Table 1). Crude oils with variable physical properties were collected mainly from the west (well LN1), the

Table 1
Sample list, geological information and spectroscopic data

Sample	Well	Depth (m)	Formation[a]	Type	QGF Intensity	QGF Index	λ_{max}	δ_λ	TSF Intensity	TSF R1 cf	TSF Em	Hydrocarbon inclusion abundance
1OF	LN10	5801.4	O	FI oils from carbonate	n/a	n/a	n/a	n/a	413	3.4	380	very high
2OF	LN44	5296.1	O	FI oils from carbonate	n/a	n/a	n/a	n/a	130	2.8	373	very high
3TF	LN2	4892	T	FI oils from sandstones	43	7.6	428	180	32	2.4	365	high
4TF	LN2	4748.04	T	FI oils from sandstones	54	9.6	425	172	78	2.9	373	high
5O	LN1	5038–5052	O	Crude oil	50	102	436	181	39	4	378	n/a
6O	LN10	5349–5381	O	Crude oil	210	80	415	134	57	1.5	348	n/a
7O	LN30	5301–5325	O	Crude oil	697	35	360	82	106	1.06	344	n/a
8C	LN22	5090–5130	C	Crude oil	162	7.9	360	69	82	0.86	341	n/a
9T	LN1	4912–4920	T	Crude oil	137	158	422	139	28	1.8	363	n/a
10T	LN3	4881–4887	T	Crude oil	45	140	416	212	160	2.5	368	n/a

QGF Intensity: the integrated area of a QGF spectrum normalised to the intensity at 300 nm.
QGF Index: the average spctral intensity between 375 nm ($I_{375\ nm}$) and 475 nm ($I_{475\ nm}$) normalised to the spectral intensity at 300 nm.
λ_{max}: the wavelength in nm corresponding to the maximum spectral intensity (I_{max}).
δ_λ: the difference of the wavelength in nm between the wavelengths corresponding to half spectral maximum intensity (1/2 I_{max}) on the spectra.
TSF Intensity: the photometer counts corresponding to every excitation/emission pair.
TSFR1: the emission intensity at 360 nm over 320 nm when excited using 270 nm UV light.
TSF Em: the emission wavelength associated with the TSF Maximum value (peak).
n/a: not applies.
[a] O: Ordovician; C: Carboniferous; T: Triassic.

middle (wells LN3 and LN30) and the east (wells LN10 and LN22) of these two fault-horst belts (Fig. 1 and Table 1). In order to select suitable samples for Molecular Composition of Inclusion (MCI) analysis, the Quantitative Grain Fluorescence (QGF; Liu and Eadington, 2005) and Total Scanning Fluorescence (TSF; Liu et al., 2005) techniques were carried out to screen the samples. Then, oil extracted from quartz was analysed using the off-line MCI protocols (George et al., in press). Samples were mechanically and chemically disintegrated, and quartz grains were separated from other lithologies using magnetic and heavy liquid separation. Potential contamination on the quartz grains was removed using successive treatments of hydrogen peroxide, hot chromic acid, Aqua Regia and organic solvents. Carbonate FI samples were disintegrated into 1–2 mm grains and then treated with organic solvent (methanol and dichloromethane) to remove contamination. Samples were not crushed until they were deemed clean following a final outside (surface) rinse. The cleaned samples were then crushed under solvent (dichloromethane) to release oil from the inclusions into the solvent.

Crude oil samples were separated into aliphatic and aromatic hydrocarbon fractions using column chromatography. The FI oil samples, outside rinses, system blanks and crude oil fractions were analysed by gas chromatography-mass spectrometry (GC-MS) using an AutoSpecQ system. The GC was fitted with a DB5MS 60 m fused silica column (i.d. 0.25 mm, film thickness 0.25 μm). GC-MS data were acquired in full scan (50–550 amu) mode and by single ion monitoring (SIM) and metastable reaction monitoring (MRM) experiments. The GC oven was programmed in two ways for different GC-MS runs: (1) an initial temperature of 40 °C for 2 min, followed by heating at 4 °C/min to 310 °C (held for 30 min); (2) an initial temperature of 40 °C for 2 min, followed by heating at 20 °C/min to 200 °C and then a second heating ramp at 2 °C/min to 310 °C (held for 30 min). GC program (2) was only used for the analysis of aliphatic biomarkers; other aliphatic and

aromatic hydrocarbons were assessed using GC program (1).

4. Results and discussion

4.1. Quantitative grain fluorescence and total scanning fluorescence

The QGF and TSF methods are rapid and cost-effective screening techniques for selecting suitable samples for MCI analysis (Liu and Eadington, 2005; Liu et al., 2005). Four samples were selected based on the TSF and QGF parameters (Table 1). The selected samples contain abundant oil inclusions, as demonstrated by a plot of TSF intensity versus *n*-alkane yields, which shows that *n*-alkane yields in this study are much higher than the cut-off value needed for reliable geochemical analysis (Fig. 3). QGF (λ_{max}, δ_λ) and TSF (R1, Em) results for the Triassic-hosted FI oils (Table 1) also suggest a close resemblance with the Triassic crude oils. Generally, less mature oils would have a longer QGF Lambda-max (λ_{max}), larger delta Lambda (δ_λ), larger TSF R1values and longer TSF Em values. Hence, the FI oils in this study also appear to be slightly less mature than the crude oils. TSF spectrograms (not shown) indicate that the Ordovician-hosted FIs and Ordovician crude oils are quite different, but that the Triassic-hosted FIs and the Triassic crude oils are similar.

4.2. n-Alkanes and acyclic isoprenoids

n-Alkane yields from the LN2 sandstone FI oil samples and LN10 and LN44 carbonate FI oil samples are around two to three orders of magnitude higher than the associated system blanks (Table 2). Most of the inclusion oil samples previously analysed at CSIRO contained 100–4000 ng *n*-alkanes/g quartz, and recovery >40 ng/g is generally regarded to be reliable (George et al., 2001a). Therefore, the results in this study give us confidence in the quality of the data.

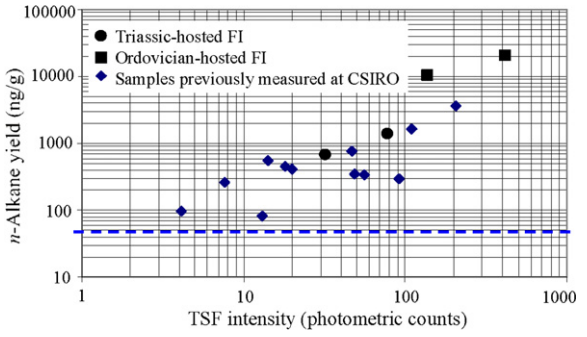

Fig. 3. Correlation of total scanning fluorescence (TSF) intensities and *n*-alkane yields, showing that the TSF method is a quick screening method for selecting samples suitable for MCI analyses. MCI data are generally reliable and easily interpreted above the dashed line (George et al., 2001a).

The FI oil samples have a smooth carbon number distribution of *n*-alkanes with a maximum between *n*-C_{17} and *n*-C_{20} (Fig. 4). The crude oil samples are lighter than the FI oil samples, with *n*-alkanes maximizing at *n*-C_{14}, except for the LN30 oil. This suggests that the crude oils are more thermally mature than the FI oils. The carbon number preference indices (CPI_{26-32}) are all near unity. Pristane/phytane (Pr/Ph; Table 2) ratios of the Ordovician-hosted FI oils (1.2) are slightly higher than those of the Triassic-hosted FI oils (0.85–1.02) and most of the crude oils (0.76–0.87), which may indicate a somewhat more oxic depositional environment for the source rock of the Ordovician-hosted FI oils (Didyk et al., 1978).

4.3. Aliphatic biomarkers

The Triassic-hosted FI oils contain higher relative abundance of C_{23} tricyclic terpane compared to other tricyclic terpanes and to hopanes than the Ordovician-hosted FI oils (Table 2). Abundant C_{23} tricyclic terpane commonly occurs in oil samples from marine source rocks (Aquino Neto et al., 1983). In contrast, the Ordovician-hosted FI oils contain more of the C_{19} tricyclic terpane and C_{24} tetracyclic terpane than the Triassic-hosted FI oils and most of the crude oils, as is shown by a plot of $C_{19}/(C_{19}+C_{23})$ tricyclic terpanes versus C_{24} tetracyclic /(C_{24} tetracyclic + C_{23} tricyclic) terpanes (Fig. 5). This likely indicates a difference in source input between Triassic-hosted FI oil, crude oils and Ordovician-hosted FI oils, although a maturity influence cannot be rule out (Farrimond et al., 1999). C_{19} and C_{20} tricyclic terpanes and C_{24} tetracyclic terpane tend to be more abundant in terrigenous-derived oils (Philp and Gilbert, 1986; Preston and Edwards, 2000; Peters et al., 2005), but the lack of higher-plant input to the likely Palaeozoic sources of the Ordovician-hosted FI oils suggests an alternative but currently unknown source is responsible. The amount of C_{24} tetracyclic terpane may also depend on organic facies lithology, with relatively high concentrations in oils from carbonate or evaporitic source rocks (Palacas, 1984; Connan

Table 2
Aliphatic hydrocarbon parameters for the FI oils and crude oils from the Lunnan Low Uplift

	1OF	2OF	3TF	4TF	5O	6O	7O	8C	9T	10T
ng C_{12-32} *n*-alkanes/g quartz crushed	5362	911	267	659	n.d.	n.d.	n.d.	n.d.	n.d.	n.d.
ng C_{12-32} *n*-alkanes recovered in FI oil	88625	7764	3810	8487	n.d.	n.d.	n.d.	n.d.	n.d.	n.d.
ng C_{12-32} *n*-alkanes recovered in system blank	4.2	0.7	3.5	10.8	n.d.	n.d.	n.d.	n.d.	n.d.	n.d.
Pr/Ph[a]	* 1.22	1.24	1.02	0.85	0.76	0.85	0.84	1.15	0.78	0.87
CPI_{26-32}[a]	1.00	0.96	1.00	0.98	0.98	0.97	–	–	1.00	1.02
C_{23} tricyclic terpane/C_{30} αβ hopane[b]	* 0.45	0.38	0.73	1.02	0.67	3.4	3.5	4.2	1.23	1.25
C_{24} tetracyclic terpane/C_{26} tricyclic terpanes[b]	* 2.8	27.9	0.89	0.78	0.77	0.73	0.69	0.86	0.59	0.80
C_{24} tetracyclic terpane/(C_{24} tetracyclic terpane + C_{23} tricyclic terpane)[b]	0.60	0.71	0.23	0.22	0.23	0.22	0.18	0.17	0.18	0.24
C_{19}/(C_{19} + C_{23}) tricyclic terpanes[b]	* 0.59	0.64	0.21	0.17	0.11	0.24	0.27	0.52	0.12	0.20
C_{29} tricyclic terpanes/(C_{29} tricyclic terpanes + C_{30} αβ hopane)[b]	* 0.32	0.03	0.29	0.29	0.24	0.61	0.51	0.46	0.34	0.36
Ts/(Ts + Tm)	0.82	0.77	0.57	0.45	0.33	0.81	0.68	0.82	0.37	0.55
C_{29}Ts/(C_{29}Ts + C_{29} αβ hopane)	0.48	0.39	0.05	0.16	0.11	0.48	0.27	0.40	0.14	0.17
C_{29}*/C_{29} αβ hopane	0.33	0.07	0.06	0.04	0.04	0.13	0.09	0.10	0.04	0.08
C_{30}*/C_{30} αβ hopane	* 0.24	0.03	0.08	0.05	0.04	0.13	0.06	0.10	0.04	0.06
C_{29} αβ hopane/C_{30} αβ hopane[b]	* 0.59	0.77	0.72	0.88	0.90	0.68	0.66	0.58	0.93	0.85
C_{29} 25-norhopane/C_{29} αβ hopane	0.00	0.00	0.08	0.12	0.18	0.16	0.09	0.13	0.17	0.08
C_{29} αβ/(αβ + βα) hopanes	0.93	0.94	0.92	0.95	0.94	0.91	0.93	0.91	0.95	0.94
C_{30} αβ/(αβ + βα) hopanes	0.96	0.95	0.94	0.96	0.95	0.95	0.94	0.94	0.95	0.96
C_{31} αβ 22*S*/(22*S* + 22*R*) hopanes	0.55	0.60	0.60	0.57	0.57	0.56	0.61	0.57	0.58	0.59
% C_{35} of total αβ homohopanes[b]	1.7	0.84	4.6	4.2	12.2	18.2	8.7	21	10.0	11.3
C_{35}/C_{34} homohopanes[b]	* 0.20	0.35	0.59	0.58	1.00	0.85	1.40	1.25	0.99	0.92
Homohopanes/C_{30} αβ hopane[b]	1.25	0.75	1.6	1.7	2.5	2.6	1.25	2.4	2.3	2.3
Gammacerane/C_{30} αβ hopane	* 0.01	0.04	0.05	0.06	0.08	0.03	0.10	0.08	0.06	0.05
28,30-BNH/C_{30} αβ hopane	* 0.02	0.03	0.15	0.07	0.06	0.08	0.04	0.07	0.06	0.07
C_{29} steranes/C_{29} αβ hopane[c]	* 0.82	0.04	0.81	0.65	0.87	3.2	1.7	1.9	1.02	1.21
C_{27}: C_{28} : C_{29} αββ steranes 20*S* + *R* (%)[d]	* 26:19:55	17:15:68	26:12:62	27:14:59	27:19:54	29:21:50	33:22:45	43:20:37	29:20:51	31:22:47
C_{30}/(C_{27} + C_{28} + C_{29} + C_{30}) ααα 20*R* steranes (%)	1.02	1.14	0.43	0.75	0.82	1.6	0.72	3.2	0.46	0.61
C_{27} + C_{28} + C_{29} βα diasteranes/(ααα + αββ steranes)	0.48	0.34	0.47	0.43	0.33	0.83	0.91	1.22	0.45	0.48
C_{29} αββ/(αββ + ααα) steranes	0.61	0.56	0.59	0.57	0.58	0.61	0.59	0.55	0.61	0.58
C_{29} ααα 20*S*/(20*S* + 20*R*) steranes	0.45	0.50	0.45	0.50	0.48	0.50	0.47	0.42	0.49	0.54
Family	3[e]	3[e]	1[e]	1[e]	1[e]	2[e]	2[e]	2[e]	1[e]	1[e]

Ratios were calculated from MRM data, (*m*/*z* $M^+ \rightarrow$ 191, 217, 259 for hopanes, steranes and diasteranes, respectively), except for m/z values in footnotes a–d.

[a] (*m*/*z* 85).

[b] (*m*/*z* 191).

[c] (*m*/*z* 217 and m/z 191).

[d] (*m*/*z* 218).

[e] Families were determined by hierarchical cluster analysis.

[*] These parameters were selected for hierarchical cluster analysis.

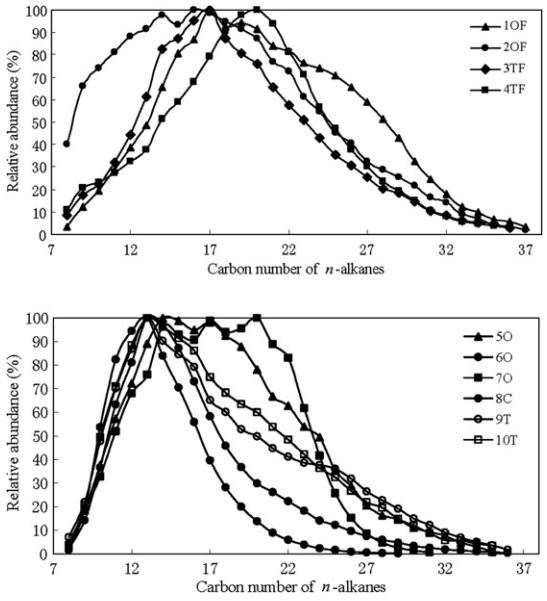

Fig. 4. Normalised *n*-alkane distribution (m/z 85 data) for FI oils (top) and crude oils (bottom) from the Lunnan Low Uplift.

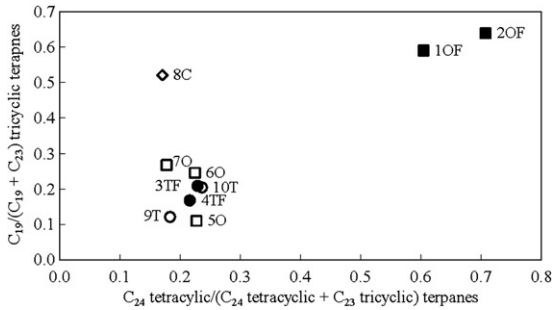

Fig. 5. Plot of C_{24} tetracyclic/(C_{24} tetracyclic + C_{23} tricyclic) terpanes versus C_{19}/(C_{19} + C_{23}) tricyclic terpanes showing that the Ordovician and Triassic-hosted crude oils correlate with the Triassic-hosted FI oils.

et al., 1986). In this case, abundant C_{24} tetracyclic terpane in the Ordovician-hosted FI oils is interpreted to indicate carbonate or evaporitic source rock lithology.

The hopane distribution of all samples is dominated by C_{30} 17(α)-hopane. The most significant difference between the Ordovician and Triassic-hosted FI oils is that the former contain more Ts and C_{29}Ts than the Triassic-hosted FI oils (Table 2). The Ts/(Ts + Tm) and C_{29}Ts/(C_{29}Ts + C_{29} αβ hopane) ratios could be influenced by both thermal maturity (Moldowan et al., 1986, 1994; Sofer et al., 1986) and depositional environment (Peters et al., 2005). The Ordovician-hosted FI oils contain less abundant

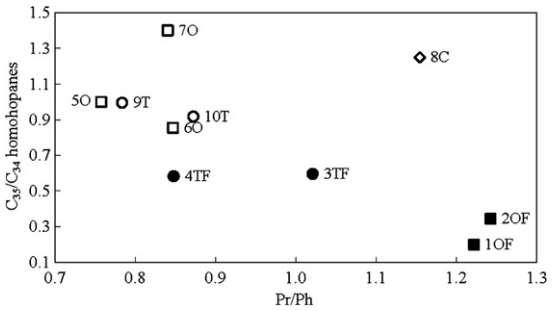

Fig. 6. Plot of Pr/Ph versus C_{35}/C_{34} homohopanes showing that the Triassic-hosted FI oils and crude oils were derived from a more reducing source rock than the Ordovician-hosted FI oils.

C_{35} homohopanes than the Triassic-hosted FI oils and the crude oils, as shown by the plot of Pr/Ph versus C_{35}/C_{34} homohopanes (Fig. 6). This indicates a less reducing (higher Eh) source rock for the Ordovician-hosted FI oils compared to the other samples (Peters et al., 2005). The gammacerane/C_{30} αβ hopane ratios and the relative abundance of 28,30-bisnorhopane are higher for the Triassic-hosted FI oils and the crude oils than for the Ordovician-hosted FI oils (Table 2), consistent with a more reducing environment for the former (Mello et al., 1988; Sinninghe Damsté et al., 1995).

The Triassic-hosted FI oils and all crude oils contain not only moderate amounts of C_{29} 25-norhopane and 25,30-bisnorhopane, but also C_{30} and C_{31} 25-norhopanes, whereas the Ordovician-hosted FI oils do not contain C_{29} 25-norhopane, and contain very little 25,30-bisnorhopane. This means that the Triassic-hosted FI oils and all crude oils show indicators of an episode of severe biodegradation (Volkman et al., 1983), whereas such a biodegradation event is not evident in the Ordovician-hosted FI oils.

The regular sterane distributions for all of the samples are similar, with $C_{29} > C_{27} > C_{28}$ steranes (Table 2). High relative abundances of C_{29} steranes compared to C_{27} and C_{28} steranes commonly indicates higher-plant input (Czochanska et al., 1988), but are also found in many Palaeozoic oils, which pre-date the radiation of land plants (Grantham, 1986). C_{30} steranes, diagnostic compounds for marine organic input (Moldowan et al., 1990), are abundant in all of the FI oils and crude oils, as detected by m/z 414 → 217 MRM transitions.

The Ordovician and Triassic-hosted FI oils and the Triassic oils have lower βα diasterane/(ααα + αββ) sterane ratio than most of the Ordovician and Carboniferous crude oils (Table 2). Higher diasterane contents indicate more acidic, clay-rich

source rocks, but are also likely influenced by higher maturity (Seifert and Moldowan, 1978). The samples with high diasterane content (mostly the Ordovician and Carboniferous crude oils) differ from those with high rearranged hopane (Ts, C_{29}Ts) content (Ordovician-hosted FI oils), possibly because rearranged hopane content is being controlled primarily by Eh, whereas diasterane content is being controlled by acidity (Moldowan et al., 1994).

The biomarker thermal maturity ratios, such as C_{29} $\alpha\beta/(\alpha\beta+\beta\alpha)$ hopanes, C_{30} $\alpha\beta/(\alpha\beta+\beta\alpha)$ hopanes, C_{31} $\alpha\beta$ $22S/(22S+22R)$ hopanes, C_{29} $\alpha\beta\beta/(\alpha\beta\beta+\alpha\alpha\alpha)$ sterane and C_{29} $\alpha\alpha\alpha$ $20S/(20S+20R)$ are at or near the equilibrium values for all samples (Table 2), indicating that the main phase of oil generation has been reached.

4.4. Aromatic hydrocarbons

Many of the common aromatic hydrocarbons occur in the samples, including alkylbenzenes, alkylnaphthalenes, alkylphenanthrenes, alkyldibenzothiophenes and arylisoprenoids. These provide further information on the thermal maturity and source characteristics of the samples.

Arylisoprenoids have previously been noted in crude oils and asphaltene pyrolysates from the Tabei Uplift (Peng and Lü, 2002; Sun et al., 2003), and were detected in all FI oils and crude oils in this study. Arylisoprenoids are diagenetic products from aromatic carotenoids produced by *Chlorobiaceae*, which are anaerobic, photosynthetic, green sulphur bacteria (Summons and Powell, 1986, 1987). The Triassic-hosted FI oils and crude oils contain abundant 1-alkyl-2,3,6-arylisoprenoids, with distributions dominated by C_{14}, C_{18} and C_{19} homologues. The relative abundance of the arylisoprenoids can be measured by the C_{14} 1-alkyl-2,3,6-arylisoprenoid/1,2,3,5-tetramethylbenzene (TeMB) ratio, which for the Triassic-hosted FI oils and crude oils is 0.28–0.54 (Table 3). The Ordovician crude oil from the most western well of the study area (LN1) has the highest value for this ratio (0.60), whilst the Ordovician-hosted FI oils and the other crude oils have lower ratios (0.04–0.11). The Triassic-hosted FI oils and crude oils also have more 1,2,3,4-TeMB than Ordovician-hosted FI oils and other oils, in which 1,2,3,5-TeMB dominates. Abundant 1,2,3,4-TeMB indicates a contribution of diaromatic carotenoids to the kerogen (Hartgers et al., 1994). Abundant arylisoprenoids and 1,2,3,4-TeMB in the Triassic-hosted FI oils and crude oils indicate a strongly reducing depositional environment for the source rock, with input from photosynthetic, green sulphur bacteria (Summons and Powell, 1986, 1987; Xinke et al., 1990; Schwark and Püttmann, 1990). The Ordovician-hosted crude oil from LN1 is more akin to the Triassic FI oils and crude oil than to the Ordovician and Carboniferous FI oils and crude oils from the eastern part of the study area.

Dibenzothiophene/phenanthrene (DBT/P) ratios are variable but are low for most samples (0.12–0.7), indicating little sulphur in the oils. The DBT versus Pr/Ph plot of Hughes et al., 1995 (not shown) indicates that most of the samples fall around the boundary of Zones 2 and 3, indicating oil derived from a low sulphur marine source rock. The exception is the LN44 Ordovician-hosted FI oil, which contains more dibenzothiophene than phenanthrene and is thus sulphur-rich (Table 3).

Several alkylnaphthalene (Radke et al., 1982b, 1994; van Aarssen et al., 1999), alkylphenanthrene (Radke et al., 1982b, 1984; Radke and Welte, 1983; Kvalheim et al., 1987) and alkyldibenzothiophene (Radke et al., 1986; George et al., 2001b) thermal maturity ratios were applied to the oils in the study. Most of the maturity-related parameters based on alkylnaphthalenes and alkylphenanthrenes show that (1) the crude oils are more mature than the FI oils, and (2) that the Ordovician-hosted and Triassic-hosted FI oils have a similar maturity (Table 3 and Fig. 7). These trends are exemplified by the methylnaphthalene ratio, the ethylnaphthalene ratio and the dimethylnaphthalene ratio-1, three ratios based on methylphenanthrenes, the dimethylphenanthrene ratio and by the dimethyldibenzothiophene ratio (Table 3). The methyldibenzothiophene, trimethylnaphthalene, tetramethylnaphthalene and alkylbiphenyl ratios do not appear to be sensitive to the maturity variations in this sample set.

Care must be applied when using published calibrations of these ratios with other maturity parameters, such as vitrinite reflectance. Calibrations often vary with source input and from basin to basin. For example, vitrinite reflectance equivalent (VRE) from the methylphenanthrene ratio based on a calibration published by Radke et al. (1984) in some cases overstates thermal maturity relative to similar calibrations of other ratios, and relative to other methylphenanthrene ratio calibrations (George and Ahmed, 2002). Notwithstanding these considerations, the FI oils are estimated to have thermal maturity in the early-middle part of the oil window,

Table 3
Aromatic hydrocarbon parameters for the FI oils and crude oils from the Lunnan Low Uplift

	1OF	2OF	3TF	4TF	5O	6O	7O	8C	9T	10T
MNR	1.08	1.05	1.37	1.12	1.97	1.43	1.67	1.30	1.67	1.74
ENR-1	2.0	0.57	nd	2.2	4.3	5.2	4.0	3.9	8.0	7.1
DNR-1	2.5	2.6	3.0	1.8	5.9	7.8	7.5	6.2	8.9	9.0
TNR-1	0.86	0.70	0.73	0.70	0.70	0.78	0.84	0.66	0.79	0.80
TMNr	0.68	0.69	0.72	0.69	0.68	0.70	0.76	0.70	0.70	0.73
TeMNr	0.82	0.86	0.85	0.82	0.76	0.66	0.72	0.70	0.78	0.78
MPI-1	0.61	0.37	0.51	0.56	0.71	0.75	0.75	0.72	0.86	0.88
% Rc from MPI-1	0.77	0.62	0.71	0.73	0.82	0.85	0.85	0.83	0.92	0.93
MPDF	0.40	0.38	0.42	0.41	0.43	0.49	0.49	0.50	0.51	0.47
MPR	0.86	0.91	1.02	0.94	1.04	1.25	1.31	1.50	1.32	1.17
% Rc from MPR	0.87	0.90	0.95	0.92	0.96	1.04	1.06	1.12	1.06	1.01
DPR	0.21	0.18	0.16	0.16	0.18	0.27	0.25	0.28	0.28	0.27
MBpR	6.4	15	29	105	45	6.0	7.4	8.2	21	17
3-MBp/4-MBp	1.7	2.1	2.5	3.7	2.5	2.9	2.8	2.3	2.2	2.2
Dibenzothiophene/phenanthrene	0.12	1.56	0.29	0.41	0.59	0.70	0.43	0.55	0.54	0.64
MDR	9.0	3.6	7.8	7.7	4.8	7.9	5.6	11.2	6.5	6.8
% Rc from MDR	1.16	0.77	1.08	1.07	0.86	1.08	0.92	1.33	0.99	1.00
DMDR	0.63	0.50	0.67	0.68	0.68	0.87	0.79	0.88	0.74	0.70
C_{14} aryl isoprenoid/1,2,3,4-TeMB	0.06	0.07	0.26	0.44	0.30	0.12	0.08	0.09	0.36	0.22
C_{14} aryl isoprenoid/1,2,3,5-TeMB	* 0.06	0.04	0.30	0.54	0.60	0.11	0.08	0.07	0.49	0.28
1,2,3,4-/1,2,3,5-TeMB	* 1.02	0.60	1.17	1.22	1.99	0.90	1.11	0.72	1.38	1.27

MNR: Methylnaphthalene ratio (2-MN/1-MN), Radke et al., 1982b.
ENR-1: ethylnaphthalene ratio 1 (2-EN]/1-EN), Radke et al., 1982b.
DNR-1: dimethylnaphthalene ratio 1 ([2,6- + 2,7-DMN]/1,5-DMN), Radke et al., 1982b.
TNR-1: trimethylnaphthalene ratio 1 (2,3,6-TMN/[1,4,6- + 1,3,5-TMN]), Radke et al., 1994.
TMNr: trimethylnaphthalene ratio (1,3,7-TMN/[1,3,7- + 1,2,5-TMN]), van Aarssen et al., 1999.
TeMNr: tetramethylnaphthalene ratio (1,3,6,7-TeMN/[1,3,6,7 + 1,2,5,6-TeMN]), van Aarssen et al., 1999.
MPI-1: Methylphenanthrene index 1.5*[3-MP + 2-MP]/[P + 9-MP + 1-MP]), Radke et al., 1982a.
% Rc from MPI-1 : Calculated vitrinite reflectance, 0.6*MPI-1 + 0.4, Radke and Welte, 1983.
MPDF: Methylphenanthrene distribution fraction (3-MP + 2-MP)/ $\sum$MPs), Kvalheim et al., 1987.
MPR: Methylphenanthrene ratio (2-MP/1-MP), Radke et al., 1982b.
% Rc from MPR: Calculated vitrinite reflectance, 0.99*log MPR + 0.94, Radke et al., 1984.
DPR: Dimethylphenanthrene ratio (3,5- + 2,6-DMP + 2,7-DMP)/(1,3- + 3,9- + 2,10- + 3,10-DMP + 1,6- + 2,9- + 2,5-DMP), Radke et al., 1982b.
MBpR: Methylbiphenyl ratio (3-MBp/2-MBp), Alexander et al., 1986.
MDR: Methyldibenzothiophene ratio (4-MDBT/1-MDBT), Radke et al., 1986.
% Rc from MDR: Calculated vitrinite reflectance, 0.073*MDR + 0.51, Radke et al., 1986.
DMDR: Dimethyldibenzothiophene Ratio (4,6-DMDBT/3,6- + 2,6-DMDBT), George et al., 2001b.
TeMB: Tetramethylbenzene.
nd = not determined.
* These parameters were selected for hierarchical cluster analysis.

with a VRE range of 0.62–0.77%. The crude oils are estimated to have thermal maturity at the peak of the oil window, with a VRE range of 0.82–0.93%.

5. Interpretation

5.1. Source and maturity characteristics

Crude oils in the Lunnan Low Uplift are more mature than the co-occurring FI oils. The FI oils have similar maturities to each other, based on aromatic hydrocarbon maturity-dependent parameters and the TSF results. Hence, the differences in the geochemical characteristics between the Ordovician and Triassic-hosted FI oils are mainly due to organic facies variations. Tricyclic and tetracyclic terpane distributions separate the Ordovician-hosted FI oils from the Triassic-hosted FI oils, indicating origins from different source rock or source rock facies. Source-related geochemical parameters separate the FI oils and crude oils into three families based on hierarchical cluster analysis (Fig. 8). Relationships among the oils were determined by 14

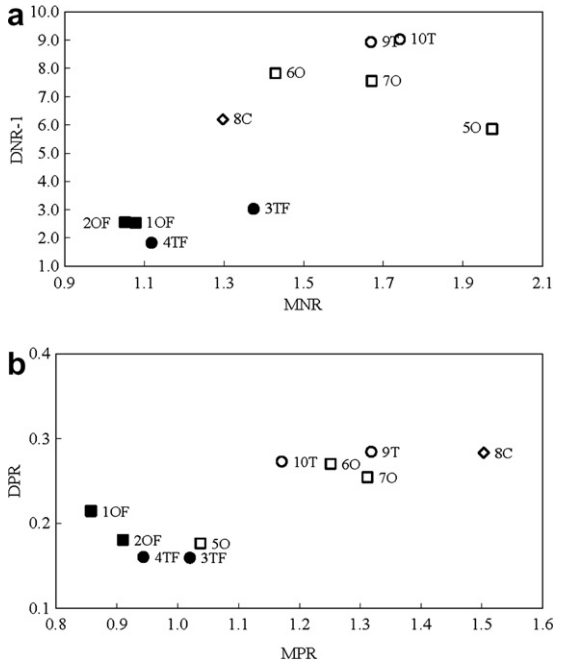

Fig. 7. Cross-plots of thermal maturity parameters, showing the higher maturity of the crude oils than the FI oils. (a) Methylnaphthalene ratio (MNR) versus dimethylnaphthalene ratio (DNR-1); and (b) methylphenanthrene ratio (MPR) versus dimethylphenanthrene ratio (DPR). For definitions of ratios see Table 3.

source-related ratios (Tables 2 and 3) which are not significantly affected by thermal maturity, migration and biodegradation.

The Ordovician and Triassic-hosted FI oils clearly are separated into different families (Fig. 8). The Triassic-hosted FI oils are interpreted to have been derived from a marine source rock deposited in a more reducing environment than the Ordovician-hosted FI oils, based on the abundance of C_{23} tricyclic terpanes, C_{35} homohopanes, 28,30-bisnorhopane and arylisoprenoids, and the lower abundance of neohopanes and the lower Pr/Ph ratios. The source rock of the Ordovician-hosted FI oils is interpreted to have been deposited in a less reducing marine depositional environment, as shown by higher Pr/Ph ratio and lesser amounts of arylisoprenoids, gammacerane, C_{35} homohopanes and 28,30-bisnorhopane. Abundant C_{24} tetracyclic terpane in the Ordovician-hosted FI oils is consistent with a carbonate source rock (e.g. Palacas, 1984; Connan et al., 1986), although this is not corroborated by other carbonate indicators such as high C_{29}/C_{30} αβ hopane ratios.

Source biomarker data show that both Triassic crude oils and the Ordovician crude oil in well LN1 are most likely related to the Triassic-hosted

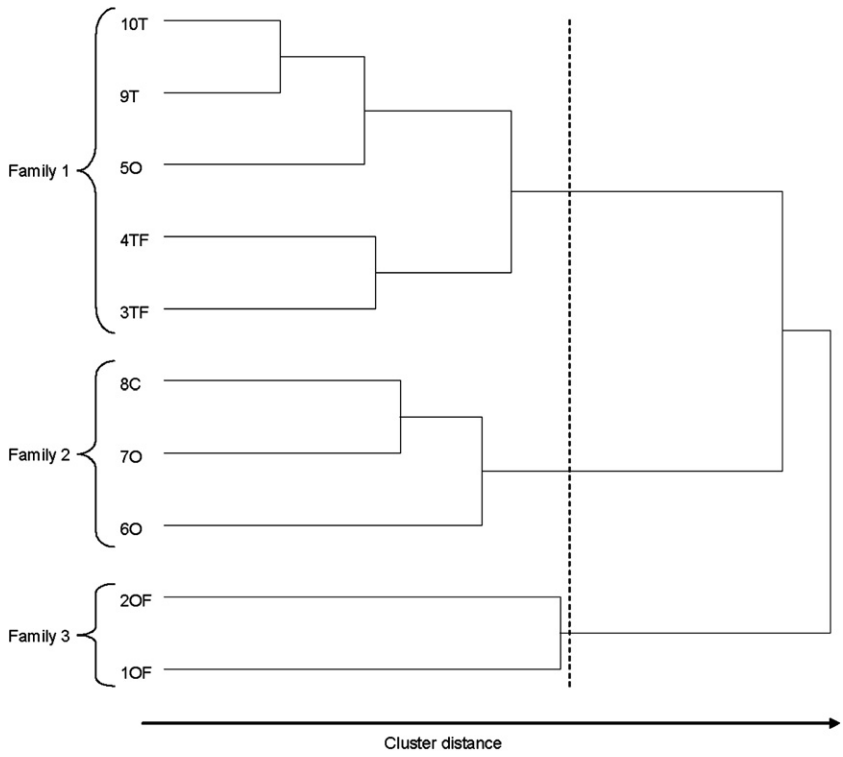

Fig. 8. Dendrogram of hierarchical cluster analysis (HCA) for selected source variables. Source variables used for calculation of Euclidian distance (autoscale preprocessing, incremental linkage) are marked by * in Tables 2 and 3.

FI oils (Fig. 8). Geochemical characteristics of other Ordovician and Carboniferous crude oils collected from the eastern part of the Lunnan Low Uplift are somewhat different to the Triassic-hosted FI oils and Triassic crude oils, but are much more different compared to the Ordovician-hosted FI oils based on hierarchical cluster analysis (Fig. 8).

5.2. Biodegradation

C_{29}–C_{31} 25-norhopanes occur in the Triassic-hosted FI oils and all of the crude oils, but not in the Ordovician-hosted FI oils. This implies that biodegradation post-dated the trapping of FI oils in the Ordovician reservoirs. The non-biodegraded Ordovician-hosted FI oils may thus represent an early charge episode. The Triassic-hosted FI oils and all of the crude oils containing 25-norhopanes also contain *n*-alkanes and acyclic isoprenoids, indicate mixing of biodegraded oil with fresher non-biodegraded oil. This kind of mixed oil may develop either during a continuous process, where the rate of biodegradation is comparable to the rate of reservoir charging, or as episodic events, where a reservoir is charged with oil which became biodegraded and then the reservoir is recharged with non-biodegraded oil. According to the burial history for the well LN1 in the western part of the study area (Fig. 9), the Triassic-hosted FI oils and all of the crude oils conform to the latter scenario. The recharge oils originated from a different source rock, based on different biomarker characteristics. The abundance of 25-norhopanes in the FI oils and the crude oils decreases from the west to the east of the Lunnan Low Uplift, implying that the palaeo-oil reservoir during the Ordovician was mainly distributed in the western part of the Lunnan Low Uplift.

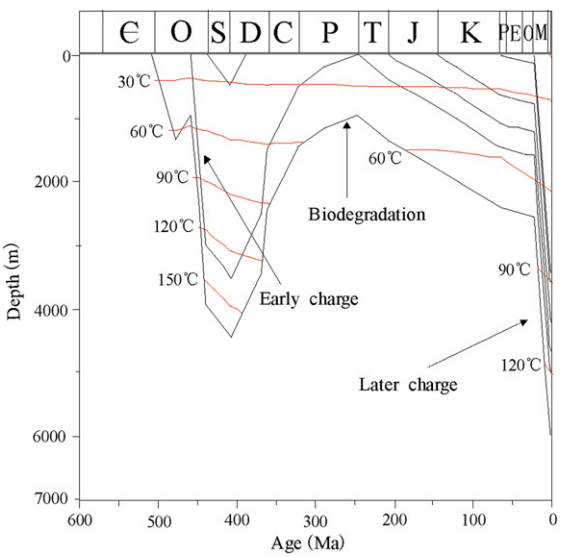

Fig. 9. Burial and thermal history model of well LN1 in the Lunnan Low Uplift. The location of well LN1 is shown in Fig. 1 (modified from Peng and Lü, 2002).

5.3. Charge history interpretation

The FI results indicate a multi-episode charge history in this region, where the composition of the oil changed as different source rocks generated hydrocarbons. The homogenisation temperature of the Ordovician inclusions is mainly 60–80 °C (Peng and Lü, 2002). Comparison with the burial and thermal history of the Ordovician reservoir in the Lunnan Low Uplift (Fig. 9) suggests that fluid inclusions in the Ordovician reservoir may have formed in the Late Ordovician and Late Devonian (Peng and Lü, 2002). Thus, an early hydrocarbon charge represented by the Ordovician-hosted FI oils most likely occurred during the Late Ordovician based on the burial history (Fig. 9). There are two known groups of source rocks in the Tarim Basin. The Cambrian-Lower Ordovician source rocks started generating oil at ~452 Ma while the Middle-Upper Ordovician source rocks started generating oil at ~150 Ma, based on the hydrocarbon generation history (Jin and Wang, 2004). Hence it is suggested that the Ordovician-hosted FI oils may have been derived from Cambrian-Lower Ordovician source rocks. Due to the presence of 25-norhopanes in the Triassic-hosted FI oils and all of the crude oils, but not in the Ordovician-hosted FI oils, the early charge is inferred to have been widely biodegraded, which is consistent with uplift and denudation from the Devonian to the Triassic. In the Permian and Triassic, the reservoir temperatures in the LN1 well were less than 60 °C, which is consistent with the temperature dependence of mesophilic microbes that operate in petroleum reservoirs (<60–80 °C) (Peters et al., 2005). Oils trapped in Ordovician inclusions, therefore, may represent the best evidence so far known of a Cambrian source rock for marine oils in the Lunnan Low Uplift.

With deposition of the overlying Mesozoic–Cenozoic sediments, large amounts of later generated hydrocarbons mixed with the early biodegraded oil during recharge to the Ordovician, Carboniferous and Triassic reservoirs. These later

charging hydrocarbons may have been generated from Middle-Upper Ordovician source rocks, according to the hydrocarbon generation history. Homogenization temperatures for Triassic-hosted FIs are mainly 90–120 °C (Peng and Lü, 2002), which means that the Triassic-hosted FIs could only have formed during the Late Tertiary, consistent with the hydrocarbon generation history of the Ordovician source rock (Jin and Wang, 2004). A number of studies document that oil inclusions are often trapped during the early stages of trap filling (e.g. Karlsen et al., 1993; Lisk et al., 1996; George et al., 1997a,b, 1998b; Isaksen et al., 1998; Bhullar et al., 1999; Volk et al., 2001, 2002). The thermal maturity of the Triassic-hosted FI oils was slightly lower than that of the pre-existing crude oils in this study, indicating initial charge of lower maturity oil that was preferentially trapped in FIs, followed by migration of increasingly mature oil from the source rock as it was buried deeper.

6. Conclusions

- Ordovician and Triassic-hosted FI oils in the Lunnan Low Uplift originated from marine source rocks having different depositional environments.
- Compared with the Triassic-hosted FI oils, the source rock for the Ordovician-hosted FI oils was deposited in a less reducing marine environment, which may have been Cambrian-Lower Ordovician in age.
- The source rock for the Triassic-hosted FI oils was deposited in a more reducing marine environment, and may have been Middle-Late Ordovician in age.
- Oil samples from the various reservoirs are largely similar to the Triassic-hosted FI oils, except that the Ordovician and Carboniferous oil samples from the eastern part of the study area contain more rearranged hopanes and diasteranes.
- Initial petroleum charge in the Lunnan Low Uplift occurred at two different times and is represented by Ordovician and Triassic-hosted FI oils.
- Ordovician-hosted FI oils provide evidence for an origin from Cambrian to Lower Ordovician source rocks. Elsewhere these oils were subsequently biodegraded due to uplift of the reservoir rocks.
- Co-existence of abundant *n*-alkanes with 25-norhopanes in the Triassic-hosted FI oils and all of the crude oils indicates that biodegradation post-dated the trapping of FI oils in the Ordovician reservoirs but not in the Triassic reservoirs.
- The crude oils are similar to the later oil charge, which played an important role in forming the oil accumulations in the Lunnan Low Uplift.

Acknowledgements

Reviewers Drs. K. Peters and M. Moldowan are gratefully acknowledged for their constructive comments that substantially improved the quality of this manuscript. We also acknowledge financial support of this work by the Project of Knowledge Innovation Program of the Guangzhou Institute of Geochemistry, the Chinese Academy of Sciences (Grant No. GIGCX-0408). We thank Manzur Ahmed for advice on sample preparation and analysis. We thank Xia Luo and Wanglu Jia for providing the oil samples.

Associate Editor—**Kenneth E. Peters**

References

Alexander, R., Cumbers, K.M., Kagi, R.I., 1986. Alkylbiphenyls in ancient sediments and petroleums. Organic Geochemistry 10, 841–845.

Aquino Neto, F.R., Trendel, J.M., Restle, A., Connan, J., Albrecht, P.A., 1983. Occurrences and formation of tricyclic and tetracyclic terpanes in sediments and petroleums. In: Bjorøy, M. et al. (Eds.), Advances in Organic Geochemistry. Wiley, Chichester, pp. 659–667.

Bhullar, A.G., Karlsen, D.A., Backer-Owe, K., Seland, R.T., Le Tran, K., 1999. Dating reservoir filling – a case history from the North Sea. Marine and Petroleum Geology 16, 581–603.

Connan, J., Bouroullec, J., Dessort, D., Albrecht, P., 1986. The Microbial input in carbonate–anhydrite facies of a sabkha palaeoenvironment from Guatemala: A molecular approach. Organic Geochemistry 10, 29–50.

Czochanska, Z., Gilbert, T.D., Philp, R.P., Sheppard, C.M., Weston, R.J., Wood, T.A., Woolhouse, A.D., 1988. Geochemical application of sterane and triterpane biomarkers to a description of oils from the Taranaki Basin in New Zealand. Organic Geochemistry 12, 123–135.

Didyk, B.M., Simoneit, B.R.T., Brassell, S.C., Eglinton, G., 1978. Organic geochemical indicators of palaeoenvironmental conditions of sedimentation. Nature 272, 216–222.

England, W.A., Mackenzie, A.S., Mann, D.M., Quigley, T.M., 1987. The movement and entrapment of petroleum fluid in the subsurface. Journal of the Geological Society London 144, 327–347.

Farrimond, P., Bevan, J.C., Bishop, A.N., 1999. Tricyclic terpane maturity parameters: response to heating by an igneous intrusion. Organic Geochemistry 30, 1011–1019.

George, S.C., Ahmed, M., 2002. Use of aromatic compound distributions to evaluate organic maturity of the Proterozoic

Middle Velkerri Formation, McArthur Basin, Australia. In: Keep, M., Moss, S.J. (Eds.), The Sedimentary Basins of Western Australia 3, Proceedings of the Petroleum Exploration Society of Australia Symposium, Perth, WA, 2002. pp. 253–270.

George, S.C., Lisk, M., Eadington, P.J., Quezada, R.A., 1998b. Geochemistry of a palaeo-oil column: Octavius 2, Vulcan Sub-basin. In: Purcell, P.G., Purcell, R.R. (Eds.), Proceedings of the Petroleum Exploration Society of Australia Symposium, Perth, WA, pp. 195–210.

George, S.C., Volk, H., Ruble, T., Lisk, M., Ahmed, M., Liu, K.Y., Quezada, R., Dutkiewicz, A., Brincat, M., Smart, S., Horsfield, B., 2001a. Extracting oil from fluid inclusions for geochemical analyses: size matters! In: Abstract of the 20th International Meeting on Organic Geochemistry, 10–14 September 2001, Nancy, France, P/TUE1/37, pp. 467–468.

George, S.C., Volk, H., Ahmed, M., in press. Geochemical analysis techniques and geological applications of oil-bearing fluid inclusions, with some Australian case studies. Journal of Petroleum Science and Engineering doi:10.1016/j.petrol.2005.10.010.

George, S.C., Greenwood, P.F., Logan, G.A., Quezada, R.A., Pang, L.S.K., Lisk, M., Krieger, F.W., Eadington, P.J., 1997b. Comparison of palaeo oil charges with currently reservoired hydrocarbons using molecular and isotopic analyses of oil-bearing fluid inclusions: Jabiru oil field, Timor Sea. Australian Petroleum Production and Exploration Association Journal 37 (1), 490–504.

George, S.C., Krieger, F.W., Eadington, P.J., Quezada, R.A., Greenwood, P.F., Eisenberg, L.I., Hamilton, P.J., Wilson, M.A., 1997a. Geochemical comparison of oil-bearing fluid inclusions and produced oil from the Toro Sandstone, Papua New Guinea. Organic Geochemistry 26, 155–173.

George, S.C., Lisk, M., Summons, R.E., Quezada, R.A., 1998a. Constraining the oil charge history of the South Pepper oilfield from the analysis of oil-bearing fluid inclusions. Organic Geochemistry 29, 631–648.

George, S.C., Ruble, T.E., Dutkiewicz, A., Eadington, P.J., 2001b. Assessing the maturity of oil trapped in fluid inclusions using molecular geochemistry data and visually-determined fluorescence colours. Applied Geochemistry 16, 451–473.

Graham, S.A., Brassell, S., Carroll, A.R., Xiao, X., Demaison, G., Milnight, C.I., Liang, Y., Chu, J., Hendrix, M.S., 1990. Characteristics of selected petroleum source rocks, Xinjiang Uygur autonomous region, Northwest China. American Association of Petroleum Geologists Bulletin 74, 493–512.

Grantham, P.J., 1986. The occurrence of unusual C_{27} and C_{29} sterane predominances in two types of Oman crude oil. Organic Geochemistry 9, 1–10.

Gu, Y., Luo, H., Shao, Z.B., 1998. Oil and Gas Origin and Preservation in Northern Part of Tarim Basin. Geological Publishing House, Beijing, pp. 95–98, 110–123.

Hanson, A.D., Zhang, S.C., Moldowan, J.M., Liang, D.G., Zhang, B.M., 2000. Molecular organic geochemistry of the Tarim Basin, Northwest China. American Association of Petroleum Geologists Bulletin 84, 1109–1128.

Hartgers, W.A., Sinninghe Damsté, J.S., de Leeuw, J.W., 1994. The identification of C_2 to C_4 alkylated benzenes in flash pyrolysates of kerogen, coals and asphaltenes. Journal of Chromatography 606, 211–220.

Head, I.M., Jones, D.M., Larter, S.R., 2003. Biological activity in the deep subsurface and the origin of heavy oil. Nature 426, 344–352.

He, D.F., Jia, C.Z., Liu, S.B., Pan, W.Q., Wang, S.J., 2002. Dynamics for multistage pool formation of Lunnan low uplift in Tarim Basin. Chinese Science Bulletin 47, 128–138.

Huang, D.F., Liu, B.W., Wang, T.D., Xu, Y.C., Chen, S.J., Zhao, M.J., 1999. Genetic type and maturity of Lower Palaeozoic marine hydrocarbon gases in the eastern Tarim Basin. Chemical Geology 162, 65–77.

Hughes, W.B., Holba, A.G., Dzou, L.I., 1995. The ratios of dibenzothiophene to phenanthrene and pristane to phytane as indicators of depositional environment and lithology of petroleum source rocks. Geochimica et Cosmochimica Acta 59, 3581–3598.

Isaksen, G.H., Pottorf, R.J., Jenssen, A.I., 1998. Correlation of fluid inclusions and reservoired oils to infer trap to fill history in the South Viking Grasben, North Sea. Petroleum Geoscience 4, 41–55.

Jia, C.Z., Wei, G.Q., 2002. Structural characteristics and petroliferous features of Tarim Basin. Chinese Science Bulletin 47, 1–11.

Jin, Z.J., Wang, Q.C., 2004. Recent developments in study of the typical superimposed basins and petroleum accumulation in China: Exemplified by the Tarim Basin. Science in China Series D 47 (Suppl. II), 1–15.

Karlsen, D.A., Nedkvitne, T., Larter, S.R., Bjørlykke, K., 1993. Hydrocarbon composition of authigenic inclusions: application to elucidation of petroleum reservoir filling history. Geochimica et Cosmochimica Acta 57, 3641–3659.

Kvalheim, O.M., Christy, A.A., Telnæs, N., Bjørseth, A., 1987. Maturity determination of organic matter in coals using the methylphenanthrene distribution. Geochimica et Cosmochimica Acta 51, 1883–1888.

Li, D.S., Liang, D.G., Jia, C.Z., Wang, G., Wu, Q.Z., He, D.F., 1996. Hydrocarbon accumulations in the Tarim Basin, China. American Association of Petroleum Geologists Bulletin 80, 1587–1603.

Lisk, M., George, S.C., Summons, R.E., Quezada, R.A., O'Brien, G.W., 1996. Mapping hydrocarbon charge histories: detailed characterization of the South Pepper oil field, Carnarvon Basin. Australian Petroleum Production and Exploration Association Journal 36, 445–464.

Liu, K.Y., Eadington, P.J., 2005. Quantitative fluorescence techniques for detecting residual oils and reconstruction hydrocarbon charge history. Organic Geochemistry 36, 1023–1036.

Liu, K., George, S.C., Li, S., Pang, X., Fenton, S., Volk, H., Ahmed, M., 2005. Total Scanning Fluorescence (TSF) as an effective screening tool for delineating oil families. In: González-Vila, F.J., González-Pérez, J.A., Almendros, G. (Eds.), Abstract Book 22nd International Meeting on Organic Geochemistry, vol. 2. EAOG: Seville, pp. 1128–1129.

Li, M.W., Xiao, Z.Y., Snowdon, L.R., Lin, R.Z., Wang, P.R., Hou, D.J., Zhang, L.Y., Zhang, S.C., Liang, D.G., 2000. Migrated hydrocarbon in outcrop samples: revised petroleum exploration directions in the Tarim Basin. Organic Geochemistry 31, 599–603.

Li, X.D., Zhang, G.Y., Tian, Z.J., 1999. Tarim Basin Oil and Gas System and Its Oil and Gas Distribution. Geological Publishing House, Beijing, pp. 54-66.

Lü, X.X., Jin, Z.J., Zhou, X.Y., Yang, N., Wang, Q.H., Pan, W.Q., 2004. Petroleum enrichment characteristics in Ordovician carbonates in Lunnan area of Tarim Basin. Chinese Science Bulletin 49, 60–65.

Mello, M.R., Telnaes, N., Gaglianone, P.C., Cheicarelli, M.I., Brassell, S.C., Maxwell, J.R., 1988. Organic geochemical characterisation of depositional palaeoenvironments of source rocks and oils in Brazilian marginal basins. Organic Geochemistry 13, 31–45.

Moldowan, J.M., Fago, F.J., Lee, C.Y., Jacobson, S.R., 1990. Sedimentary 24-*n*-propylcholestanes, molecular fossils diagnostic of marine algae. Science 247, 309–312.

Moldowan, J.M., Peters, K.E., Carlson, R.M.K., Schoell, M., Abu-Ali, M.A., 1994. Diverse applications of petroleum biomarkers maturity parameters. The Arabian Journal for Science and Engineering 19, 273–298.

Moldowan, J.M., Sundararaman, P., Schoell, M., 1986. Sensitivity of biomarker properties to depositional environment and/or source input in the Lower Toarcian of S.W. Germany. Organic Geochemistry 10, 915–926.

Palacas, J.G., 1984. Carbonate rocks as sources of petroleum: geological and chemical characteristics and oil-source correlationProceedings of the Eleventh World Petroleum Congress 1983, vol. 2. John Wiley & Sons, Chichester, UK, pp. 31–43.

Peng, P.A., Lü, X.X., 2002. Diversity of sources, reservoir formation periods and crudes in Lunnan area. Study report of the project on "Formation, distribution and enrichment rules for oil and gas in superimposed basins in China" for the state 973 project. Guangzhou Institute of Geochemistry, Chinese Academy of Sciences, 126–128.

Peters, K.E., Walters, C.C., Moldowan, J.M., 2005. The Biomarker Guide, Biomarkers and Isotopes in Petroleum Exploration and Earth History. Cambridge University Press, Cambridge, pp. 566–567.

Philp, R.P., Gilbert, T.D., 1986. Biomarker distributions in Australian oils predominantly derived from terrigenous source material. Organic Geochemistry 10, 73–84.

Preston, J.C., Edwards, D.S., 2000. The petroleum geochemistry of oils and source rocks from the northern Bonaparte Basin, offshore northern Australia. The APPEA Journal 40, 257–282.

Radke, M., Leythaeuser, D., Teichmüller, M., 1984. Relationship between rank and composition of aromatic hydrocarbon for coals of different origins. Organic Geochemistry 6, 423–430.

Radke, M., Rullkötter, J., Vriend, S.P., 1994. Distribution of naphthalenes in crude oils from the Java Sea: source and maturation effects. Geochimica et Cosmochimica Acta 58, 3675–3689.

Radke, M., Welte, D.H., 1983. The methylphenanthrene index (MPI); a maturity parameter based on aromatic hydrocarbons. In: Bjorøy, M. et al. (Eds.), Advances in Organic Geochemistry 1981. Wiley, Chichester, pp. 504–512.

Radke, M., Welte, D.H., Willsch, H., 1982a. Geochemical study on a well in the Western Canada Basin: relation of the aromatic distribution pattern to maturity of organic matter. Geochimica et Cosmochimica Acta 46, 1–10.

Radke, M., Welte, D.H., Willsch, H., 1986. Maturity parameters based on aromatic hydrocarbons: Influence of the organic matter type. Organic Geochemistry 10, 51–63.

Radke, M., Willsch, H., Leythaeuser, D., Teichmüller, M., 1982b. Aromatic compounds of coal; relation of distribution pattern to rank. Geochimica et Cosmochimica Acta 46, 1831–1848.

Schwark, L., Püttmann, W., 1990. Aromatic hydrocarbon composition of the Permian Kupferschiefer in the Lower Rhine basin, NW Germany. Organic Geochemistry 16, 749–761.

Seifert, W.K., Moldowan, J.M., 1978. Applications of steranes, terpanes and monoaromatics to the maturation, migration and source of crude oils. Geochimica et Cosmochimica Acta 42, 77–95.

Sinninghe Damsté, J.S., Kenig, F., Koopmans, M.P., Köster, J., Schouten, S., Hayes, J.M., de Leeuw, J.W., 1995. Evidence for gammacerane as an indicator of water-column stratification. Geochimica et Cosmochimica Acta 59, 1895–1900.

Sofer, Z., Zumberge, J.E., Lay, V., 1986. Stable carbon isotopes and biomarkers as tools in understanding genetic relationship, maturation, biodegradation, and migration in crude oils in the Northern Peruvian Oriente (Maranon) Basin. Organic Geochemistry 10, 377–389.

Summons, R.E., Powell, T.G., 1986. Chlorobiaceae in Palaeozoic sea revealed by biological markers, isotopes and geology. Nature 319, 763–765.

Summons, R.E., Powell, T.G., 1987. Identification of aryl isoprenoids in source rocks and crude oils: Biological markers for the green sulphur bacteria. Geochimica et Cosmochimica Acta 51, 557–566.

Sun, Y.G., Xu, S.P., Lu, H., Chai, P.X., 2003. Source facies of the Paleozoic petroleum systems in the Tabei uplift, Tarim Basin, NW China: implications from aryl isoprenoids in crude oils. Organic Geochemistry 34, 629–634.

van Aarssen, B.G.K., Bastow, T.P., Alexander, R., Kagi, R.I., 1999. Distribution of methylated naphthalenes in crude oils: indicators of maturity, biodegradation and mixing. Organic Geochemistry 30, 1213–1227.

Volk, H., George, S.C., Lisk, M., Killops, S.D., Ahmed, M., Quezada, R.A., 2001. Charge histories of petroleum reservoirs in the Gippsland and Taranaki Basins Evidence from the analysis of oil inclusions and crude oils. In: Hill, K.C., Bernecker, T. (Eds.), Eastern Australasian Basins Symposium, A Refocused Energy Perspective for the Future, Petroleum Exploration Society of Australia, Special Publication, pp. 413–422.

Volk, H., George, S.C., Killops, S.D., Lisk, M., Ahmed, M., Quezada R.A., 2002. The use of fluid inclusion oils to reconstruct the charge history of petroleum reservoirs an example from the Taranaki Basin. In: Proceedings of the 2002 New Zealand Petroleum Conference, Auckland, 24–27 February 2002, Auckland, Crown Minerals, pp. 221–233.

Volkman, J.K., Alexander, R., Kagi, R.I., Woodhouse, G.W., 1983. Demethylated hopanes in crude oils and their applications in petroleum geochemistry. Geochimica et Cosmochimica Acta 47, 785–794.

Wang, T.G., Wang, C.J., Zhang, W.B., 2003. Geochemical study on formation of the Ordovician oil/gas reservoirs in Tahe oil field. Sinopec Xinxing Northwest China Branch.

Xiao, X.M., Song, Z.G., Liu, D.H., Liu, Z.F., Fu, J.M., 2000. The Tazhong hybrid petroleum system, Tarim Basin, China. Marine and Petroleum Geology 17, 1–12.

Xinke, Y., Pu, F., Philp, R.P., 1990. Novel biomarkers found in South Florida basin. Organic Geochemistry 15, 433–438.

Yang, J., Huang, H.P., Zhang, S.C., Chen, F.J., 2003. Semi-quantitative evaluation of mixed oil in northern uplift of the Tarim basin. Geochimica et Cosmochimica Acta 32, 105–111.

Zhang, K., 2000. Discussion of Ordovician oil and gas reservoir properties of Tahe Oil Field. Oil and Gas Geology of Marine Facies 5, 47.

Zhang, S.C., Hanson, A.D., Moldowan, J.M., Graham, S.A., Liang, D.G., Chang, E., Fago, F., 2000. Paleozoic oil-source rock correlations in the Tarim Basin, NW China. Organic Geochemistry 31, 273–286.

Zhang, S.C., Huang, H.P., 2005. Geochemistry of Paleozoic marine petroleum from the Tarim Basin, NW China: Part 1: Oil family classification. Organic Geochemistry 36, 1204–1214.

Zhang, S.C., Liang, D.G., Li, M.W., Xiao, Z.Y., He, Z.H., 2002. Molecular fossils and oil-source rock correlations in Tarim Basin, NW China. Chinese Science Bulletin 47, 20–27.

Zhao, M.J., Xiao, Z.Y., Peng Y., 1997. New advances in organic geochemical research concerning Tarim Basin. Report of Exploration and Research Center under the Headquarters for Petroleum Exploration in Tarim Basin, pp. 20–85.

Zhou, F.Y., Zhang, S.C., 2000. Petroleum charging history of the LN2 petroleum pool in the Lunnan area of the Tarim Basin-evidence from the fluid inclusions. Bulletin of Lithology 16, 670–676.